

ATMOSPHERIC SCIENCE

Change of extreme snow events shaped the roof of traditional Chinese architecture in the past millennium

Siyang Li^{1†}, Ke Ding^{2,3†}, Aijun Ding^{2,3*}, Lejun He^{1,4}, Xin Huang^{2,3}, Quansheng Ge^{5*}, Congbin Fu^{2,3}

As a symbol of civilization and culture, architecture was originally developed for sheltering people from unpleasant weather or other environmental conditions. Therefore, architecture is expected to be sensitive to climate change, particularly to changes in the occurrence of extreme weather events. However, although meteorological factors are widely considered in modern architecture design, it remains unclear whether and how ancient people adapted to climate change from the perspective of architecture design, particularly on a millennium time scale. Here, we show periodic change and a positive trend in roof slope of traditional buildings in the northern part of central and eastern China and demonstrate climate change adaptation in traditional Chinese architecture, driven by fluctuations in extreme snowfall events over the past thousand years. This study provides an excellent example showing how humans have long been aware of the impact of climate change on daily life and learned to adapt to it.

INTRODUCTION

Societal and cultural responses to climate change during the Holocene have been commonly addressed by integrating detailed archaeological data and paleoclimatic records (1, 2). In West Asia, North Africa, the Indus Valley, and many other preindustrial civilizations, climate change (e.g., a sudden or prolonged cooling, short-term aridification, or persistent multicentury drought) has been examined and reported as a crucial factor leading to social collapses and the demise of cultures (3–10). The Chinese civilization, known as one of the earliest civilizations worldwide, went through numerous climate change events (11), which notably affected agriculture, population, economy (12–14), and even contributed to wars, riots, and the rise and fall of dynasties (15–17). Traditional Chinese architecture is an integral component of Chinese civilization and reflects the daily life. Considering the building materials and construction systems, architecture is closely related to the natural environment, especially meteorological factors (18–20). Therefore, climate-architecture connection can demonstrate the impact of climate change and people's climatic adaptational behavior in history.

Roofs are crucial for sheltering humans from rainfall, snowfall, and sunlight, and they are the most climate-sensitive, vulnerable, and exposed parts of buildings (21, 22). Therefore, investigating the historical adjustment of roofs is likely to provide insight into the relationship between architecture design and adaptation to climate change (23). To the best of our knowledge, no previous published study has investigated this relationship on a millennium time scale. In this study, we explore the impacts of climate change on roof modification and people's acclimating behavior from a dwelling perspective based on reconstructed chronosequence of roof pitches of ~200 official architectural remains together with high-resolution

reconstructed paleoclimatic data (24, 25) in the northern part of central and eastern (NCE) China. The results suggest that the main factor driving the millennial-scale modification of roofs is the change of extreme snowfall events. This study urges greater scientific and societal attention, as we are facing escalated anthropogenic climate change that calls for affordable, reliable, and resilient climate adaptation strategies, particularly in the Global South, given their limited access to adequate climate adaptation resources.

RESULTS

Change of roof pitch over the past thousand years

Sloping and curved roofs are distinctive features of traditional Chinese architecture. They are closely related to beam structures and represent the social hierarchy and esthetics to some extent (19). Although roofs have maintained their main characteristics from prehistoric times to the present in China, their modifications can reveal particular aspects of an era (Fig. 1, A and B). The remains of official architecture in NCE China (from the mid-late Tang Dynasty to the middle term of the Qing Dynasty) form a sequential and abundant series, thereby setting a good database for this research (in other areas, remains, particularly those before Yuan Dynasty, are rare and randomly dispersed). The NCE region is in the central area of traditional Chinese culture, and it is a geographically semihumid area, with high climate sensitivity (26, 27). In other words, this location is uniquely controlled by winter and summer monsoons and affected by both the cold-dry air from the northwest and the warm-wet air from the southeast. Therefore, this area is under an amplified influence of climatic fluctuation and provides an excellent opportunity to explore the impacts of climate change on traditional Chinese architecture.

Surveys conducted in the 1930s by Liang (28) and Liang and Liu (29) and other members of the Society for the Study of Chinese Architecture have reported notable changes in roof pitches of traditional Chinese architecture [represented by the height span ratio (HSR)] (Figs. 1, A and B and 2). Several recent studies (30–32) have suggested an upward trend of HSR from ~20% in the 8th

Copyright © 2021
The Authors, some
rights reserved;
exclusive licensee
American Association
for the Advancement
of Science. No claim to
original U.S. Government
Works. Distributed
under a Creative
Commons Attribution
NonCommercial
License 4.0 (CC BY-NC).

¹School of History, Nanjing University, Nanjing 210023, China. ²School of Atmospheric Sciences, Nanjing University, Nanjing 210023, China. ³Collaborative Innovation Center for Climate Change, Nanjing 210023, China. ⁴Institute of Oriental Architecture, Nanjing University, Nanjing 210023, China. ⁵Institute of Geographic Sciences and Natural Resources Research, Chinese Academy of Science, Beijing 100101, China. *Corresponding author. Email: dingaj@nju.edu.cn (A.D.); geqs@igsnnr.ac.cn (Q.G.) †These authors contributed equally to this work.

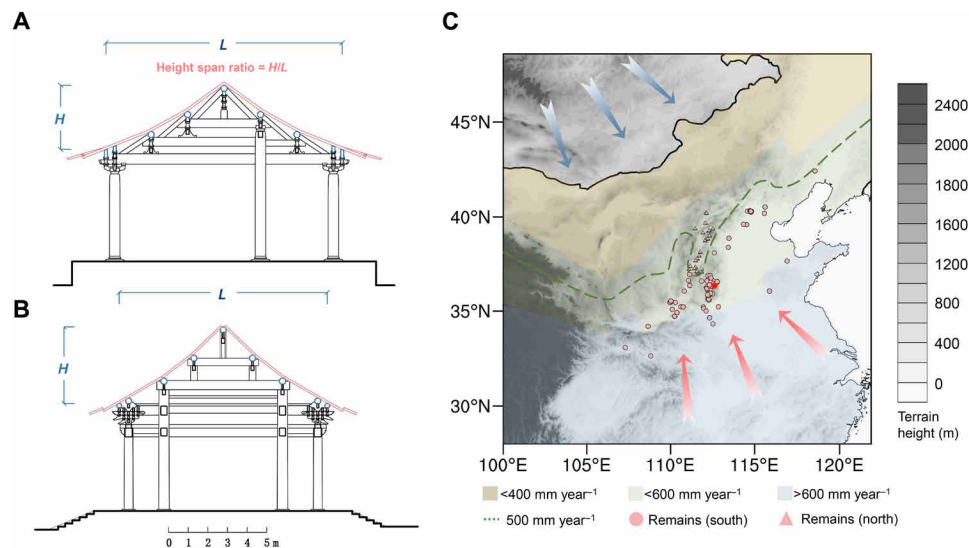


Fig. 1. Typical Chinese timber architecture and locations of building remains. Typical structure of traditional Chinese timber architecture and height span ratio (HSR) in the (A) Song Dynasty (~1103 CE) and (B) Ming and Qing Dynasties (~1600 CE). (C) Locations of remains in 750–1750 CE. The light red circles and triangles show the remains in the south (precipitation $> 500\text{ mm year}^{-1}$) and north (precipitation $< 500\text{ mm year}^{-1}$) regions. The dark red circle shows the location of the Longmen Temple. The colorful shading areas represent locations with different average precipitation. The green dashed line shows a 500-mm precipitation isohyet. The blue and red vectors indicate cold-dry and warm-wet air from north and south, respectively.

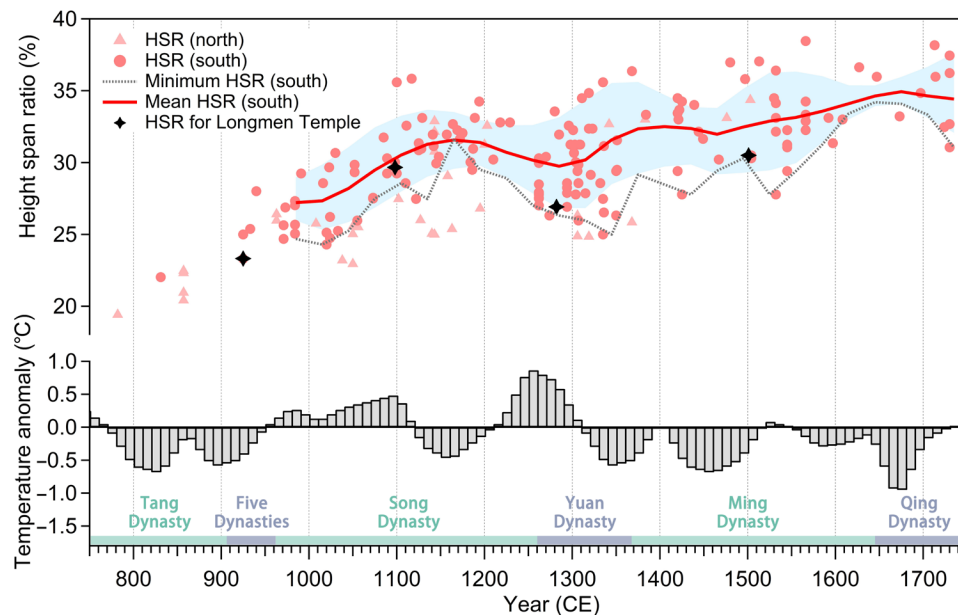


Fig. 2. Time series of HSR and air temperature anomaly in 750–1750 CE. Triangles and circles show the HSR of the remains in the north and south regions (locations definitions are shown in Fig 1), respectively. The blue shaded area marks the 5th to 95th percentile range of HSR in the south region, which was smoothed using locally weighted regression. The gray dashed and red solid lines give the minimum and mean HSR, respectively, in the south region. The black stars indicate the HSR in the Longmen Temple. The gray bars show the temperature anomaly in the winter half year in central and eastern China.

century to ~35% in the 18th century. A notable roof curvature reduction in ~1700 CE has also been reported (19, 32), along with several analyses of the causes of the esthetic changes during the Yuan Dynasty (1271–1368 CE) and technological advancement in the late Ming and early Qing dynasties (around 1600–1700 CE) (31). However, the reconstructed roof pitch chronosequence (Fig. 2;

HSR data source is given in table S1) indicates that there is a complex and nonlinear HSR variation with a century-scale fluctuation. In 1100–1200 CE and 1300–1650 CE, there was a clear increase in roof pitch, especially in the minimum HSR. However, HSR became relatively unrestricted and showed a downward trend in 1200–1300 CE, which led to smoother roofs in ~1300 CE. Therefore, a

more reasonable explanation addressing the causes of periodic HSR changes should be investigated in the research of traditional Chinese architecture. Considering the similar time scale of roof pitch fluctuation and climate change (33, 34) and the high climate sensitivity of traditional Chinese architecture, we analyzed HSR data and the reconstructed temperature in central-eastern China (24) to investigate this relationship. The region covered under the reconstructed temperature study is shown in fig. S1.

As shown in Fig. 2, the roof HSR (especially the minimum HSR) has a negative correlation with the reconstructed average temperature in the winter half year, along with a nearly 30-year delay (fig. S2). Furthermore, the Granger causality analysis (GCA) also suggests that temperature anomaly is the Granger cause of the roof pitch change with a time lag of 30 years (see Materials and Methods). In cold periods, roofs became steeper [1100–1200 CE and 1300–1750 CE, which corresponds to the Little Ice Age (35)], whereas, in warm periods, the roof pitch descended notably [1200–1300 CE, which corresponds to the Medieval Warm Period in Europe (8)]. Previous studies have shown a 30-year lag between climate change and the related responses in human society (7). Considering this delay, the negative correlation between roof pitch and reconstructed temperature suggests an influence of climate change on the design of traditional Chinese architecture.

This cold-steeper and warm-smoother correspondence is reflected not only in the long-term data but also in individual cases. A notable example is the Longmen Temple in Pingshun, Shanxi Province (Fig. 3 and fig. S3). Four of its five major buildings have a relatively clear construction/reconstruction time for different warm and cold periods in 925–1504 CE. These buildings well represent the HSR trend in different ages (black stars in Fig. 2). According to the historical document of building standards of the Song Dynasty (*Yingzao fashi*, 1103 CE) (36), these four buildings in the Longmen Temple were supposed to have a nearly identical roof pitch of ~27%. However, the two buildings constructed in cold periods presented steeper roofs, at 29.67% (1098 CE) and 30.50% (1498–1504 CE), whereas the one in the warm period was smoother, at 26.92% (1271–1294 CE) [historical records indicate that it was already

cold and snowy in central China before 1098 CE (37, 38); details are shown in table S2]. This case study illustrates that the cold-steeper and warm-smoother correlation is a remarkable phenomenon, and roof pitches tend to respond efficiently to environmental demands instead of simply pursuing the harmony and coordination of an architectural complex, which is considered essential in traditional Chinese architecture. The low HSR value of the building in 925 CE might be attributed to technical limitations. We will analyze this example at the end of the following section because it may reflect the technological advancement under the influence of climate change.

Driving factors of roof pitch changes associated with climate change

Considering the negative correlation between air temperature and roof HSR, the role of climate change in this relationship should be further investigated. It is known that roofs have the primary function of sheltering from sunshine, wind, and precipitation, including snow in winter. First, as enclosed buildings, no evidence shows that roof pitch influences indoor air temperature. Second, in NCE China, it is generally wet in the warm period and dry in the cold period (27, 39, 40). Therefore, if rainfall was the main factor driving roof pitch modification, then roofs would become steeper in warmer periods to increase drainage capacity, which is inconsistent with the observed trend and oscillations. Last, considering that these buildings located in a semihumid area of NCE China where the weather is relatively cold in winter, snow load is likely to be an influential factor in roof designing because of the close relationship between roof pitch and snow-removal capacity, which is seen in American, Canadian, European, and Chinese building standards (41–45). Furthermore, historical literatures have reported the damage and collapse of traditional buildings by heavy snow, causing economic losses and casualties (46). Therefore, we hypothesized that the fluctuation of snowfall intensity had caused the modification of roof pitch in the past thousand years.

To verify our hypothesis, we first examined whether roof pitch was correlated with snowfall. Because of the lack of quantitative

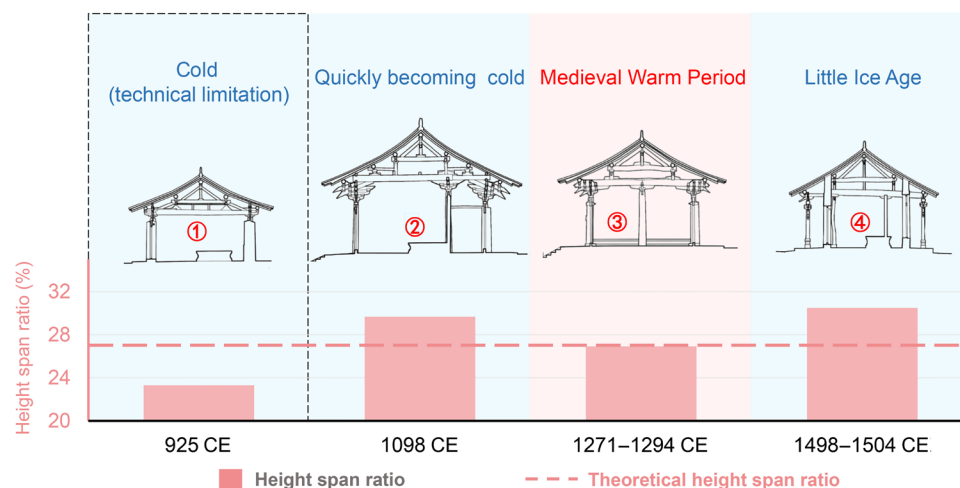


Fig. 3. HSR Variations in 925–1504 CE in the Longmen Temple. The building designs show that the four buildings belong to different warm and cold periods. The red bars indicate the corresponding HSR, and the red dashed line indicates the theoretical HSR. The HSR of different buildings is also shown in Fig. 2. The location of the Longmen Temple and the layout of the buildings are shown in Fig. 1 and fig. S3, respectively.

snowfall data in history, we used modern reanalysis data from 1981 to 2019. The method is reasonable because, in that area, snowfall intensity strongly depends on local terrain (47), which indicates that the current relative intensity of snowfall could be similar to that of the past thousand years, considering that the topography has not substantially changed in the millennium scale. We selected the period of 1110–1210 CE, when climate became significantly cold owing to the weakening of solar radiation and volcanic eruption (48, 49), to quantify the relationship between snowfall and roof pitch (see Materials and Methods). We observed that the roof pitch of building remains (which were constructed in the same cold period and are geographically close, at different topographic positions) was positively correlated with snowfall intensity (fig. S4). As the snowfall increased from ~ 0.2 to ~ 0.35 mm day⁻¹, the roof HSR increased from ~ 25 to $\sim 35\%$. This result indicates that snowfall is the most important driving force of roof pitch diversity. Meanwhile, modern architectural research shows that a stronger snow-removal capacity can be obtained for HSR higher than 23.33% in China (45), which is also consistent with our analysis of traditional Chinese architecture and technically supports the conjecture of the roof pitch–snowfall intensity relationship. Furthermore, the HSR difference caused by snowfall is similar to the HSR difference from the late Five Dynasties to the middle term of the Qing Dynasty (950 CE to 1750 CE) (Fig. 2), which further supports that the change in snowfall caused by climatic fluctuation may be an essential factor driving the modification of roof pitches over the past thousand years.

Before statistically assessing this correspondence between climate change and roof pitch modification, a proxy of estimated snowfall intensity anomaly should be developed to address the absence of reconstructed quantitative historical snowfall data in China. By analyzing nearly 40 years of reanalysis data, we observed that the snowfall significantly increased in cold years in north China (fig. S5A). On the basis of the reconstructed winter half-year temperature anomaly and a deduced quantitative relation of -0.074 mm day⁻¹ K⁻¹ between snowfall and air temperature (using reanalysis data from 1989 to 2019, shown in fig. S5B), we roughly estimated the snowfall intensity anomaly from 950 CE to 1750 CE (see Materials and Methods). This estimation, as shown in Fig. 4, agrees well with the snowfall events anomaly data developed by Chu *et al.* (25) based on statistics of snowfall events in historical documents (the region with snowfall events is shown in fig. S1). There was almost no snowfall record for the warm period in ~ 1300 CE, whereas, for the Little Ice Age in 1300–1750 CE, the continuous reduction of temperature in the winter half year was accompanied by a sharp increase in recorded snowfall events (50), which suggests that the decrease in temperature and increase in snowfall are generally in phase in central and eastern China on a centennial scale.

Combining the statistically estimated snowfall anomaly and the quantitative relation between snowfall intensity and roof pitch, we further estimated the snow-driven minimum HSR from 950 CE to 1750 CE (see Materials and Methods). As shown in Fig. 4, there is a considerably close correspondence between the minimum HSR estimated and the minimum HSR of building remains. In addition, the estimated minimum HSR exactly reproduced the turning points of the minimum HSR values around 1180, 1270, 1430, 1490, 1540, and 1690 CE. The consistency between measured and estimated minimum HSR indicates that the fluctuation of snowfall intensity owing to climate change is an essential factor driving the modification of roof pitch over the past thousand years. During the warm periods,

roof pitches tended to be more unrestricted because of the lower snowfall intensity, and, accordingly, they showed a wider range and downward trend of roof HSR. In cold periods, heavier snowfall led to steeper roofs of newly built houses, aiming to remove the snow more efficiently and avoid future damage. This conclusion was further confirmed by the reduction in roof curvature in ~ 1700 CE (corresponding to the Little Ice Age, when the technique for building roofs improved) (19, 31, 32), as a less curved roof also enhances the snow-removal capacity. From another perspective, the statistical roof pitch provides us a method to quantify the snowfall changes during cold periods, which is difficult to obtain from numerical models and commonly used proxy records of paleoclimate such as tree rings and stalagmites. As for the relatively large bias between the estimated and measured minimum HSR from 1550 CE to 1750 CE, we assumed that the difference derives from the underestimation of extreme snowfall intensity (51–53) and shortage of HSR data.

One could argue that ancient people would have rebuild their roofs to adapt to the increasing snowfall intensity in cold periods if the snowfall anomaly was the main factor leading to roof pitch modification. This contradictory situation was attributed to the economic cost of roof construction, which represents up to half of the total labor and material costs of a traditional Chinese building (36). Therefore, repairing became a regular choice for damaged or deformed roofs, whereas the design and construction of steeper roofs were applied only to new buildings constructed during the cold periods, thereby characterizing the observed oscillations of roof pitches. One may also wonder why Chinese people did not maintain steeper roofs to avoid possible damage even in warm periods. That can be attributed to costs and the diverse need for sunshine and rainfall sheltering. In addition, another possible explanation considers the study of a collective memory of natural disasters, which suggests that people remember a catastrophe for one to two generations. The knowledge of an event is then likely to fade away, and people start behaving in the same manner as they did before the disaster (54). Furthermore, this time span of memory and knowledge could explain the delay in the modifications of roof HSR (Fig. 4) compared to the temperature fluctuations. Therefore, our analysis indicates that the abnormal snowfall caused by climate change is the main factor driving the modification of roof pitches within the development of traditional Chinese architecture over the past thousand years.

Technology and esthetics are also important factors that may influence roof designs (31, 32). We attempted to clarify the possible influence from these factors through specific cases. As shown in Fig. 2, the upward trend of roof pitch in 750–940 CE (cold period) was consistent with the cold-steeper hypothesis. However, similar to the building in 925 CE in the Longmen Temple, the HSR values before 940 CE presented an overall linear trend and were systematically lower than those in the later period. Upon analyzing the typical structure of buildings, we speculated that technical limitations may have been the cause of a restricted HSR range. As shown in fig. S6, the HSR increased from 19.24% in 782 CE to 29.67% in 1098 CE, and the roof structure became more complex, for instance, the relative position of the main girder went from below to above the eave-purlin since ~ 940 CE (55). This structural improvement notably facilitated the construction of steeper roofs and was gradually applied in later buildings. Considering the weak snow-removal capacity of roofs for lower HSR (e.g., 23.33% as a critical point) (45), the positive trend of HSR may suggest that people in the cold period

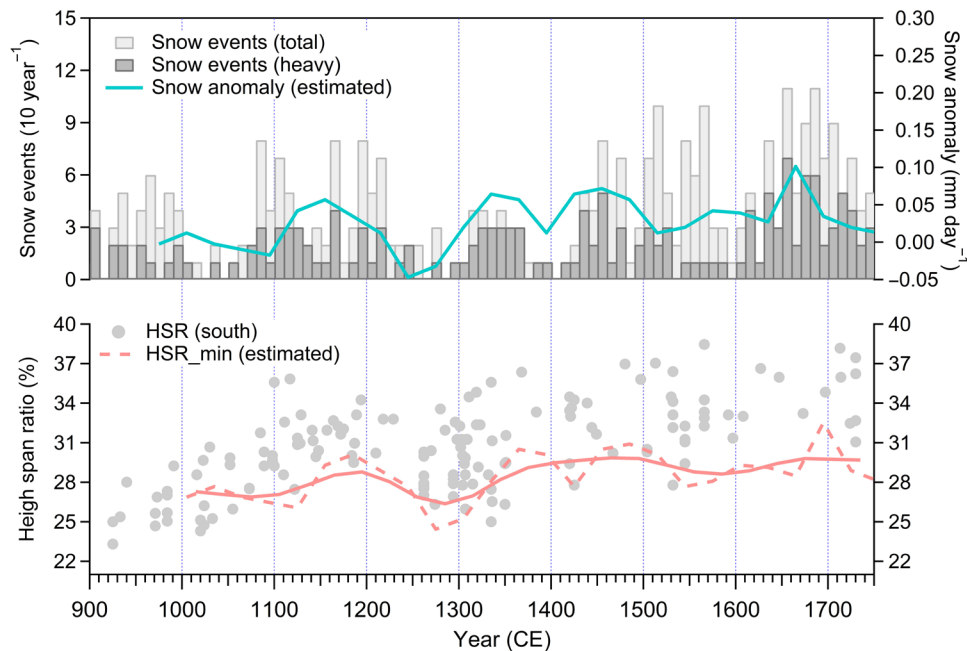


Fig. 4. Estimated and observed snowfall and HSR data. The light and dark gray bars in the (Top) indicate the number of total and heavy snow events in historical records in central and eastern China, and the cyan line shows the estimated snowfall anomaly. (Bottom) The gray dots and red dashed line show the HSR of the remains and the estimated minimum HSR in the south region, respectively. The red solid line gives the trend of the estimated minimum HSR, which was smoothed using locally weighted regression. Note that Snowfall anomaly is given as water equivalent height, which represents the water depth if the snow melted evenly.

before 940 CE were also willing to build steeper roofs but were limited by technical factors. The impact of technical limitation may last several decades, which can explain the relatively large bias between the estimated and observed minimum HSR before 1050 CE (Fig. 4). Another case is, at the beginning of the freezing period in ~1700 CE, a relatively new and more convenient roof design method replaced the old one and allowed people to create steeper and less curved roofs (31, 32), which further enhanced their snow-removal capacity. These examples suggest that climate change is an essential factor driving people to improve their building technology for a better adaptation to environmental factors.

We also noticed that the trend of maximum HSR was different from that of minimum HSR (Fig. 4). For example, in ~1300 AD, the minimum HSR decreased noticeably, while the maximum HSR presented only a slight decrease. This difference may have been driven by esthetic factors or traditions: Chinese people have a strong respect for tradition and tend to follow the esthetic tradition unless there is a strong demand or pressure. Nevertheless, the changes made as an adaptation to the environment may also become part of the esthetic tradition in later generations. For example, along with the revolution of the roof design method in ~1700 CE, the new regulation for roof construction was written in the official construction code (*Gongcheng zuofa*) and was completed in the 1730s and followed by the new official buildings during the Qing Dynasty (19).

DISCUSSION

Roof modifications throughout different periods have been generally attributed to esthetic habits or improvement in building technology. However, this study has identified a nonmonotonic increase in roof

HSR based on ~200 remains over a millennium. We quantitatively reveal that the main factor driving the modification of roof pitch and curvature of official buildings in NCE China was the fluctuation in snowfall intensity associated with climate change over the past thousand years. The responses of roof modification to the climatic fluctuations indicate an intelligent long-term adaptive behavior of the ancient Chinese. They adjusted their buildings for a more stable and suitable roof formation when faced with various weather extremes caused by climate change. It also indicates that notable esthetic changes and technological advancements in buildings were also associated with the demands caused by climate change.

This study suggests that the designs of buildings or even cities should comprehensively consider adaptation to future environmental changes (56). In addition to the direct heating impact of global warming, the increasing occurrence of extreme weather events—including heavy snow, drought, flood, and other natural disasters—is another severe problem that should be addressed (57, 58). To reduce the losses caused by extreme weather events, designers should carefully consider local climate and natural disasters according to climate prediction (59). Furthermore, as the intensity of extreme events is commonly underestimated by recent models (60), the urban and architectural design codes should be stricter and comprehensively address the increasing number of extreme events. Specifically, in developing countries, where wood is widely used as a primary building material, governments should consider adaptive strategies for building designs, as timber architecture is more vulnerable and sensitive to climate change. Reinforcing or rebuilding with new materials that are more economical and adaptive to the harsh natural environment may be a feasible solution to mitigate the impacts of climate change (61).

MATERIALS AND METHODS**Statistics of roof HSR**

We separated the north and south HSR data because the warm and wet southerly wind easily forms precipitation on the southward windward slope. As shown in Fig. 1C, the precipitation mainly follows the terrain height and is always higher on the windward slope to the south than in the valley (47). This difference in precipitation resulted in different adaptational behavior of buildings. Therefore, we used the 500-mm isohyet as an index of the hydrologic cycle to separate the two regions. Although the isohyet moves northward in the warm period and retreats southward in the cold periods (40), the relative magnitude of precipitation in both regions was likely relatively stable because the topography has not substantially changed at a millennium scale.

We selected the data of the south region for the statistical analysis because the studied building remains were mainly located in the south region. To define the HSR trend in history and reduce the noise due to the relatively low amount of data, we separated the HSR data in the southern region into bins for every 30 years and smoothed the minimum (5% percentage), maximum (95% percentage) and mean values in each bin using a locally weighted regression method. To analyze the correlation between HSR and temperature anomaly, we smoothed the minimum HSR value using three-point averages when there were less than five values in a bin (~1240, 1360, and 1650 AD). The GCA was also used to examine the causal links between minimum roof pitch and temperature anomaly (62). Before implementing GCA, we detrended, standardized, and subjected the data to first-level differentiation to obtain stationary data (checked via augmented Dickey-Fuller test). The causal relationship was significant for 1030–1720 CE, with a time lag of 30 years at the 0.1 level ($P = 0.077$), which suggests that the temperature anomaly likely influenced the roof pitch.

Correlation between HSR and snowfall

To estimate the correlation between HSR and snowfall, we analyzed the HSR in 1110–1210 CE, a period with freezing temperatures and more available data. The snowfall was higher in the windward slope of the mountains and lower in the valleys, mainly because of the topography (fig. S4A) (47), which indicates that the snow distribution was relatively stable in history. Therefore, the snowfall data from the reanalysis data (ERA5-Land), the HSR values of roofs on the mountains and valleys, were used to quantify the roof snow load (fig. S4B). In addition, because the roof snow load is almost linearly related to roof slope (41), the relation between HSR and snowfall can be regarded as the relation between the anomaly of HSR and the anomaly of snowfall. Notably, ERA5-Land is a reanalysis dataset providing a consistent view of the evolution of land variables over several decades with a resolution of 0.1°. Furthermore, the snowfall was described as water equivalent height, that is, the water depth if the snow had melted evenly.

Reconstructed data of snowfall anomaly and minimum HSR

To estimate the snowfall anomaly in 950–1750 CE, we used the reconstructed temperature anomaly data and the relationship between snowfall and temperature in 1981–2019 as follows

$$\text{Snowfall}_{\text{anomaly_estimate}} = R_{\text{snowfall}} \times T_{\text{anomaly}} \quad (1)$$

where $\text{Snowfall}_{\text{anomaly_estimate}}$ is the estimated snowfall anomaly; R_{snowfall} is the growth rate of snowfall with temperature in the winter half year, calculated based on reduced major axis regression for temperature and snowfall at the locations of the building remains in the south region (fig. S5B); and T_{anomaly} is the reconstructed historical temperature anomaly (24). The temperature and snowfall data used for the regression were obtained from ERA5-Land for 1981–2019.

To estimate the minimum HSR ($\text{HSR}_{\text{min_estimate}}$) in history, we selected a period to obtain a baseline of the minimum HSR (HSR_0) and snowfall anomaly (Snowfall_0). Subsequently, we estimated the minimum HSR by

$$\text{HSR}_{\text{min_estimate}} = \text{HSR}_0 + \text{HSR}_{\text{anomaly_snow_driven}}(\text{delay } 30 \text{ y}) \quad (2)$$

where $\text{HSR}_{\text{anomaly_snow_driven}}$ is the anomaly of the minimum HSR driven by the snowfall change. We delayed $\text{HSR}_{\text{anomaly_snow_driven}}$ by 30 years because of the 30-year lag between climate change and the respective responses in human society (7). The variable $\text{HSR}_{\text{anomaly_snow_driven}}$ was calculated by

$$\text{HSR}_{\text{anomaly_snow_driven}} = (\text{Snowfall}_{\text{anomaly_estimate}} - \text{Snowfall}_0) \times R_{\text{HSR}} \quad (3)$$

where R_{HSR} is the growth rate of HSR with snowfall, which was calculated using reduced major axis regression for snowfall and HSR for 1110–1210 CE, as described in the previous section (fig. S4B). This method was used to estimate the minimum HSR driven only by the influence of snowfall anomaly.

SUPPLEMENTARY MATERIALS

Supplementary material for this article is available at <https://science.org/doi/10.1126/sciadv.abh2601>

REFERENCES AND NOTES

1. H. Weiss, R. S. Bradley, Archaeology: What drives societal collapse? *Science* **291**, 609–610 (2001).
2. P. B. DeMenocal, Cultural responses to climate change during the late Holocene. *Science* **292**, 667–673 (2001).
3. H. Weiss, M.-A. Courty, W. Wetterstrom, F. Guichard, L. Senior, R. Meadow, A. Curnow, The genesis and collapse of third millennium north Mesopotamian civilization. *Science* **261**, 995–1004 (1993).
4. M. Staubwasser, F. Sirocko, P. M. Grootes, M. Segl, Climate change at the 4.2 ka BP termination of the Indus valley civilization and Holocene south Asian monsoon variability. *Geophys. Res. Lett.* **30**, 1425 (2003).
5. D. A. Hodell, J. H. Curtis, M. Brenner, Possible role of climate in the collapse of Classic Maya civilization. *Nature* **375**, 391–394 (1995).
6. U. Büntgen, W. Tegel, K. Nicolussi, M. McCormick, D. Frank, V. Trouet, J. O. Kaplan, F. Herzig, K.-U. Heussner, H. Wanner, J. Luterbacher, J. Esper, 2500 years of European climate variability and human susceptibility. *Science* **331**, 578–582 (2011).
7. D. D. Zhang, H. F. Lee, C. Wang, B. Li, Q. Pei, J. Zhang, Y. An, The causality analysis of climate change and large-scale human crisis. *Proc. Natl. Acad. Sci. U.S.A.* **108**, 17296–17301 (2011).
8. E. Xoplaki, D. Fleitmann, J. Luterbacher, S. Wagner, J. F. Haldon, E. Zorita, I. Telelis, A. Toreti, A. Izdebski, The Medieval Climate Anomaly and Byzantium: A review of the evidence on climatic fluctuations, economic performance and societal change. *Quat. Sci. Rev.* **136**, 229–252 (2016).
9. E. Xoplaki, J. Luterbacher, S. Wagner, E. Zorita, D. Fleitmann, J. Preiser-Kapeller, A. M. Sargent, S. White, A. Toreti, J. F. Haldon, L. Mordechai, D. Bozkurt, S. Akçer-Ön, A. Izdebski, Modelling climate and societal resilience in the Eastern Mediterranean in the last millennium. *Hum. Ecol.* **46**, 363–379 (2018).
10. F. C. Ljungqvist, A. Seim, H. Huhtamaa, Climate and society in European history. *Wiley Interdiscip. Rev.-Clim. Chang.* **12**, e691 (2020).
11. D. Jiang, G. Yu, P. Zhao, X. Chen, J. Liu, X. Liu, S. Wang, Z. Zhang, Y. Yu, Y. Li, L. Jin, Y. Xu, L. Ju, T. Zhou, X. Yan, Paleoclimate modeling in China: A review. *Adv. Atmos. Sci.* **32**, 250–275 (2015).

12. C.-B. An, L. Tang, L. Barton, F.-H. Chen, Climate change and cultural response around 4000 cal yr B.P. in the western part of Chinese Loess Plateau. *Quatern. Res.* **63**, 347–352 (2005).
13. S. Yu, C. Zhu, J. Song, W. Qu, Role of climate in the rise and fall of Neolithic cultures on the Yangtze Delta. *Boreas* **29**, 157–165 (2000).
14. U. Büntgen, V. S. Myglan, F. C. Ljungqvist, M. McCormick, N. D. Cosmo, M. Sigl, J. Jungclaus, S. Wagner, P. J. Krusic, J. Esper, J. O. Kaplan, M. A. C. de Vaan, J. Luterbacher, L. Wacker, W. Tegel, A. V. Kiryanov, Cooling and societal change during the Late Antique Little Ice Age from 536 to around 660 AD. *Nat. Geosci.* **9**, 231–236 (2016).
15. X. Fang, W. Yu, Progress in the studies on the phenological responding to global warming. *Adv. Earth Sci.* **17**, 714–719 (2002).
16. Q. Ge, H. Liu, J. Zheng, L. Xiao, The climate change and social development over the last two millennia in China. *Chinese J. Nat.* **35**, 9–21 (2013).
17. D. D. Zhang, P. Brecke, H. F. Lee, Y.-Q. He, J. Zhang, Global climate change, war, and population decline in recent human history. *Proc. Natl. Acad. Sci. U.S.A.* **104**, 19214–19219 (2007).
18. J. M. Fitch, D. P. Branch, Primitive architecture and climate. *Sci. Am.* **203**, 134–144 (1960).
19. S. Liang, *A Pictorial History of Chinese Architecture: A Study of the Development of its Structural System and the Evolution of its Types*, W. Fairbank, Ed. (MIT Press, 1984).
20. D. P. Fang, S. Iwasaki, M. H. Yu, Q. P. Shen, Y. Miyamoto, H. Hikosaka, Ancient Chinese timber architecture. I: Experimental study. *J. Struct. Eng.* **127**, 1348–1357 (2001).
21. V. Meløyund, K. R. Lisø, J. Siem, K. Apeland, Increased snow loads and wind actions on existing buildings: Reliability of the Norwegian building stock. *J. Struct. Eng.* **132**, 1813–1820 (2006).
22. M. Abuseif, Z. Gou, A review of roofing methods: Construction features, heat reduction, payback period and climatic responsiveness. *Energies* **11**, 3196 (2018).
23. T. van Hooff, B. Blocken, J. Hensen, H. Timmermans, On the predicted effectiveness of climate adaptation measures for residential buildings. *Build. Environ.* **82**, 300–316 (2014).
24. Q. Ge, J. Zheng, X. Fang, Z. Man, X. Zhang, P. Zhang, W.-C. Wang, Winter half-year temperature reconstruction for the middle and lower reaches of the Yellow River and Yangtze River, China, during the past 2000 years. *Holocene* **13**, 933–940 (2003).
25. G. Chu, Q. Sun, X. Wang, J. Sun, Snow anomaly change from historical documents in eastern China during the past two millennia and implication for low-frequency variability of AO/NAO and PDO. *Geophys. Res. Lett.* **35**, L14806 (2008).
26. L. Tan, Y. Cai, Z. An, H. Cheng, C.-C. Shen, S. F. M. Breitenbach, Y. Gao, R. L. Edwards, H. Zhang, Y. Du, A Chinese cave links climate change, social impacts, and human adaptation over the last 500 years. *Sci Rep* **5**, 12284 (2015).
27. J. Chen, F. Chen, S. Feng, W. Huang, H. Liu, A. Zhou, Hydroclimatic changes in China and surroundings during the Medieval Climate Anomaly and Little Ice Age: Spatial patterns and possible mechanisms. *Quat. Sci. Rev.* **107**, 98–111 (2015).
28. S. Liang, A study on the Guanyin Pavilion and Gate of Dule Temple (in Chinese). *Bull. Soc. Res. Chinese Archt.* **7**, 1–92 (1932).
29. S. Liang, D. Liu, Survey on the traditional buildings in Datong (in Chinese). *Bull. Soc. Res. Chinese Archt.* **12**, 1–168 (1933).
30. M. Chen, in *The Study of System of Carpentry Work in Construction Method* (in Chinese) (Cultural Relics, Beijing, 1981), pp. 183–192.
31. X. Fu, D. Guo, X. Liu, G. Pan, Y. Qiao, D. Sun, *Chinese Architecture* (Yale Univ. Press, City of New Haven, 2002).
32. H. Guo, in *The System of Major Carpentry in Official Buildings of Ming Dynasty* (in Chinese) (Southeast Univ. Press, Nanjing, 2005), pp. 52.
33. Z. An, G. Wu, J. Li, Y. Sun, Y. Liu, W. Zhou, Y. Cai, A. Duan, L. Li, J. Mao, H. Cheng, Z. Shi, L. Tan, H. Yan, H. Ao, H. Chang, J. Feng, Global monsoon dynamics and climate change. *Annu. Rev. Earth Planet. Sci.* **43**, 29–77 (2015).
34. Z. An, S. C. Clemens, J. Shen, X. Qiang, Z. Jin, Y. Sun, W. L. Prell, J. Luo, S. Wang, H. Xu, Y. Cai, W. Zhou, X. Liu, W. Liu, Z. Shi, L. Yan, X. Xiao, H. Chang, F. Wu, L. Ai, F. Lu, Glacial-interglacial Indian summer monsoon dynamics. *Science* **333**, 719–723 (2011).
35. J. Luterbacher, D. Dietrich, E. Xoplaki, M. Grosjean, H. Wanner, European seasonal and annual temperature variability, trends, and extremes since 1500. *Science* **303**, 1499–1503 (2004).
36. S. Liang, *Notes on Yingzao fashi* (in Chinese) (China Architecture & Building, Beijing, 1983).
37. Q. Ge, in *Climate Change Through Every Chinese Dynasty* (in Chinese) (Science Press, Beijing, 2010), pp. 393–394.
38. D. Zhang, in *A Compendium of Chinese Meteorological Records of the Last 3,000 Years* (in Chinese) (Jiangsu Education Publishing House, Nanjing, 2013), pp. 424–426.
39. J. Liu, B. Wang, H. Wang, X. Kuang, R. Ti, Forced response of the East Asian summer rainfall over the past millennium: Results from a coupled model simulation. *Climate Dynam.* **36**, 323–336 (2011).
40. F. Chen, J. Chen, W. Huang, S. Chen, X. Huang, L. Jin, J. Jia, X. Zhang, C. An, J. Zhang, Westerlies Asia and monsoonal Asia: Spatiotemporal differences in climate change and possible mechanisms on decadal to sub-orbital timescales. *Earth Sci. Rev.* **192**, 337–354 (2019).
41. D. A. Taylor, Roof snow loads in Canada. *Can. J. Civ. Eng.* **7**, 1–18 (1980).
42. National Research Council of Canada, “National Building Code of Canada” (National Research Council of Canada, 2005).
43. American Society of Civil Engineers, “Minimum Design Loads for Buildings and Other Structures (ASCE/SEI 7–10)” (American Society of Civil Engineers, 2013).
44. “Eurocode 1-Actions on Structures, Part 1–3: General Actions, Snow Loads”, (London: Standards Policy and Strategy Committee, 2003).
45. Ministry of Construction of the People’s Republic of China, “GB50009–2001 Load code for 408 building structures” (China Architecture & Building, Beijing, 2002).
46. Z. Song, in *Chronology of Major Natural Disasters and Anomalies in Ancient China* (in Chinese) (Guangdong Education, Guangzhou, 1992), pp. 203–204.
47. Y. Li, H. Zhi, D. Zhang, Analysis of temporal and spatial distribution and large-scale circulation features of extreme weather events in Shanxi Province, China in recent 30 years. *J. Geosci. Environ. Protect.* **7**, 160–176 (2019).
48. M. Sigl, M. Winstrup, J. R. McConnell, K. C. Welten, G. Plunkett, F. Ludlow, U. Büntgen, M. Caffee, N. Chellman, D. Dahl-Jensen, H. Fischer, S. Kipfthul, C. Kostick, O. J. Maselli, F. Mekhaldi, R. Mulvaney, R. Muscheler, D. R. Pasteris, J. R. Pilcher, M. Salzer, S. Schüpbach, J. P. Steffensen, B. M. Vinther, T. E. Woodruff, Timing and climate forcing of volcanic eruptions for the past 2,500 years. *Nature* **523**, 543–549 (2015).
49. C. Oppenheimer, Ice core and palaeoclimatic evidence for the timing and nature of the great mid-13th century volcanic eruption. *Int. J. Climatol.* **23**, 417–426 (2003).
50. P. Wang, X. Fang, L. He, Historical records on cold events and their influence during 1328–1330 AD in China. *J. Palaeogeogr.* **6**, 480–484 (2004).
51. K. S. Jennings, T. S. Winchell, B. Livneh, N. P. Molotch, Spatial variation of the rain–snow temperature threshold across the Northern Hemisphere. *Nat. Commun.* **9**, 1148 (2018).
52. D. Zhang, Y. Liang, A study of the severest winter of 1670/1671 over china as an extreme climatic event in history. *Adv. Clim. Change Res.* **13**, 25–30 (2017).
53. J.-H. Yan, H.-L. Liu, Z.-X. Hao, X.-Z. Zhang, J.-Y. Zheng, Climate extremes revealed by Chinese historical documents over the middle and lower reaches of the Yangtze River in winter 1620. *Adv. Clim. Change Res.* **5**, 118–122 (2014).
54. V. Fanta, M. Šálek, P. Sklenicka, How long do floods throughout the millennium remain in the collective memory? *Nat. Commun.* **10**, 1105 (2019).
55. D. He, in *Comprehensive Studies on Early Southeast Territory of Shanxi Province* (in Chinese) (Cultural Relics, Beijing, 2015), pp. 153–240.
56. J. G. Carter, G. Cavan, A. Connelly, S. Guy, J. Handley, A. Kazmierczak, Climate change and the city: Building capacity for urban adaptation. *Prog. Plan.* **95**, 1–66 (2015).
57. X. Wang, D. Jiang, X. Lang, Future extreme climate changes linked to global warming intensity. *Sci. Bull.* **62**, 1673–1680 (2017).
58. R. K. Pachauri, M. R. Allen, V. R. Barros, J. Broome, W. Cramer, R. Christ, J. A. Church, L. Clarke, L. Dahe, P. Dasgupta, N. K. Dubash, O. Edenhofer, I. Elgizouli, C. B. Field, P. Forster, P. Friedlingstein, J. Fuglested, L. Gomez-Echeverri, S. Hallegatte, G. Hegerl, M. Howden, K. Jiang, B. Jimenez Cisneros, V. Kattsov, H. Lee, K. J. Mach, J. Marotzke, M. D. Mastrandrea, L. Meyer, J. Minx, Y. Mulugetta, K. O’Brien, M. Oppenheimer, J. J. Pereira, R. Pichs-Madruga, G.-K. Plattner, H.-O. Pörtner, S. B. Power, B. Preston, N. H. Ravindranath, A. Riahi, M. Rusticucci, R. Scholes, K. Seyboth, Y. Sokona, R. Stavins, T. F. Tschakert, P. van Vuuren, J.-P. Ypersele, “Climate Change 2014: Synthesis Report. Contribution of Working Groups I, II and III to the Fifth Assessment Report of the Intergovernmental Panel on Climate Change”, (IPCC, 2014).
59. C. B. Field, V. R. Barros, D. J. Dokken, K. J. Mach, M. D. Mastrandrea, T. E. Bilir, M. Chatterjee, K. L. Ebi, Y. O. Estrada, R. C. Genova, B. Girma, E. S. Kissel, A. N. Levy, S. Mac Cracken, P. R. Mastrandrea, L. L. White, *Climate Change 2014-Impacts, Adaptation and Vulnerability: Part A: Global and Sectoral Aspects: Volume 1, Global and Sectoral Aspects: Working Group II Contribution to the IPCC Fifth Assessment Report* (Cambridge Univ. Press, 2014).
60. J. Schewe, S. N. Gosling, C. Reyher, F. Zhao, P. Ciais, J. Elliott, L. Francois, V. Huber, H. K. Lotze, S. I. Seneviratne, M. T. H. van Vliet, R. Vautard, Y. Wada, L. Breuer, M. Büchner, D. A. Carozza, J. Chang, M. Coll, D. Deryng, A. de Wit, T. D. Eddy, C. Folberth, K. Friedler, A. D. Friend, D. Gerten, L. Gudmundsson, N. Hanasaki, A. Ito, N. Khabarov, H. Kim, P. Lawrence, C. Morfopoulos, C. Müller, H. M. Schmied, R. Orth, S. Ostberg, Y. Pokhrel, T. A. M. Pugh, G. Sakurai, Y. Satoh, E. Schmid, T. Stacke, J. Steenbeek, J. Steinkamp, Q. Tang, H. Tian, D. P. Tittensor, J. Volkholz, X. Wang, L. Warszawski, State-of-the-art global models underestimate impacts from climate extremes. *Nat. Commun.* **10**, 1–14 (2019).
61. T. G. Nijland, O. C. Adan, R. P. Van Hees, B. D. van Etten, Evaluation of the effects of expected climate change on the durability of building materials with suggestions for adaptation. *Heron* **54**, 37–48 (2009).
62. C. W. J. Granger, Investigating causal relations by econometric models and cross-spectral methods. *Econometrica* **37**, 424–438 (1969).
63. C. Wu, C. Bai, *Traditional Architecture Measurement* (in Chinese), Q. Wang, Ed. (Tianjin Univ. Press, 2006).

64. Y. Geng, "A study on the Longmen Monastery in Pingshun and existing early monasteries in Zhuozhang River Valley (in Chinese)", thesis, Tianjin University, Tianjin (2017).

Acknowledgments: We are grateful to the ECMWF for providing ERA5-Land data and the group of G. Chu for the snow events data. We thank A. Trujillo-Ortiz and R. Hernandez-Walls for creating the program of reduced major axis regression. We also thank J. Zheng, X. Zhou, X. Zhou, X. Ma, R. An, W. Wu, S. Lou, Y. Liu, S. Zhang, X. Yang, C. Zhang, and R. Chen for contribution in data preparation and helpful discussions. **Funding:** This study was funded by the Collaborative Innovation Center for Climate Change and partly funded by the Social Science Foundation of Jiangsu Province, China (20LSC008) and Fundamental Research Funds for the Central Universities (DLTD2107). **Author contributions:** S.L., K.D., and A.D. conceived the overall idea. L.H. contributed to data collection. X.H. contributed to part of the data analysis and plots. Q.G. guided the data analysis and discussion on its relationship with past climate change. S.L. and K.D. conducted most of the analyses and wrote the manuscript together with A.D., with contributions from all authors. **Competing interests:** The authors declare that they have no competing interests. **Data and materials availability:** The reconstructed temperature anomaly data were obtained from Ge *et al.* (24), and the historical

snowfall events data were obtained from Chu *et al.* (25). The ERA5-Land data were downloaded from the website <https://cds.climate.copernicus.eu/cdsapp#!/home>. The HSR data were obtained from published papers (listed in table S1). The typical structure and HSR data in the Song Dynasty (Fig. 1A) and the Ming and Qing Dynasties (Fig. 1B) were obtained from *Yingzao fashi* (36) and Wu and Bai (63). The layout (fig. S3) and building designs (Fig. 3) of the Longmen Temple were obtained from Geng (64). The typical structure of roofs in fig. S6 was obtained from He (55). All data needed to evaluate the conclusions in the paper are present in the paper and/or the Supplementary Materials.

Submitted 25 February 2021

Accepted 19 July 2021

Published 8 September 2021

10.1126/sciadv.abh2601

Citation: S. Li, K. Ding, A. Ding, L. He, X. Huang, Q. Ge, C. Fu, Change of extreme snow events shaped the roof of traditional Chinese architecture in the past millennium. *Sci. Adv.* **7**, eabh2601 (2021).